Elementary Molecule–Surface Scattering Processes Relevant to Heterogeneous Catalysis: Insights from Quantum Dynamics Calculations

2

Cristina Díaz, Axel Gross, Bret Jackson, and Geert-Jan Kroes

Abstract

We show some examples of molecule/surface systems that have been recently described using quantum dynamics simulations, such as H_2/metal surfaces and CH_4/metal surfaces. Quantum simulations performed on these systems have yielded results in excellent agreement with independent experimental measurements. These simulations have allowed, for example, the analysis of the role of the internal degrees of freedom of the molecule, the interpretation of puzzling controversial experimental results, and the suggestion of novel experiments.

2.1 Introduction

Although we do not notice it often, in everyday life we are surrounded by phenomena involving molecule–surface interactions: for instance, the corrosion of a coin (or any other metallic object). Considering the coin, the O_2 molecules in the air interact with the metal surface atoms causing a structural damage, leaving a layer

C. Díaz (✉)
Departamento de Química, Módulo 13, Universidad Autónoma de Madrid,
28049 Madrid, Spain
e-mail: cristina.diaz@uam.es

A. Gross
Institut für Theoretische Chemie, Universität Ulm, 89069 Ulm, Germany
e-mail: axel.gross@uni-ulm.de

B. Jackson
Department of Chemistry, University of Massachusetts, Amherst, MA 01003, USA
e-mail: jackson@chem.umass.edu

G.-Jan Kroes
Leiden Institute of Chemistry, Gorlaeus Laboratories, Leiden University,
2300 RA Leiden, The Netherlands
e-mail: g.j.kroes@chem.univleiden.nl

F. Gatti (ed.), *Molecular Quantum Dynamics*, Physical Chemistry in Action,
DOI 10.1007/978-3-642-45290-1_2, © Springer-Verlag Berlin Heidelberg 2014

of oxidized material (rust) on the coin. Another example is the green appearance on the domes of some old buildings. This latter phenomenon is due to the oxidation of copper, material from which the domes are made.

Interactions of molecules with surfaces also play an important role in wide range of technologically relevant applications. For example, the dissociative adsorption of a molecule on a metal surface is the first and one of the fundamental reaction steps occurring in heterogeneous catalysis—about 90 % of the chemical manufacturing processes employed worldwide use catalysts in one form or another [10]. For example, the industrial synthesis of ammonia, from N_2 and H_2, is mediated by a hydrogenation reaction where an iron or a ruthenium surface catalyzes the reaction. Furthermore, N_2 dissociation is considered the rate-limiting step in this process. At the point, we should point out that most of the ammonia produced is used for fertilizers, making ammonia essential for our society. Another example closely related to our daily life can be found in the exhaust systems of cars, where platinum, rhodium, and palladium surfaces are used as catalysts to convert poisonous gasses expelled directly from the engine, like CO and NO_x, harmful to the environment, into a less harmful exhaust mixture of CO_2, H_2O, N_2, and O_2, before being ejected into the air. Platinum surfaces are also used as catalysts in the process of dehydrogenation of butane (C_4H_{10}) to butadiene (C_4H_6), which is used in the production of synthetic rubber or in the upgrading of the octane rating of gasoline [84]. Other examples of chemical reactions of industrial importance in which surfaces play the role of catalyst are: (1) the synthesis of methanol (CH_3OH) from CO and H_2, (2) the oxidation of ethylene to ethylene oxide, which is used in the production of antifreezes, (3) lubrication processes that influences the durability of mechanical systems, and (4) crystals growth, which determines, e.g., the quality of semiconductor devices. Special mention deserves the steam reforming process, through which methane (CH_4) and water molecules react over a Ni catalyst producing hydrogen [4, 79].[1] Due to its industrial significance, CH_4 dissociation in CH_3 and H is one of the most studied reaction in surface science [48, 60]. To conclude with this, by no means exhaustive, list of molecule/surfaces interaction processes relevant to heterogeneous catalysis we would like to point out that their importance was worldwide recognized in 2007 when the Nobel Prize in Chemistry was awarded to Gerhard Ertl for the detailed description of the sequence of elementary molecule/surface reactions by which ammonia is produced, unraveling the fundamental mechanisms of the Haber–Bosch process [25].

The reactions involved in these processes are usually too complicated to be studied in detail as a whole. Therefore surface scientists try to understand reaction mechanisms by breaking them up into simpler steps, which are studied under well-defined conditions. In this respect, accurate quantum dynamics simulations are essential to gain deeper insight into this elementary steps, and thereby to progress in modeling and improving heterogeneous catalysis. Nowadays, quantum dynamics studies including explicitly all molecular degrees of freedom (DOFs) can be

[1] Hydrogen may be considered the energy carrier of the future.

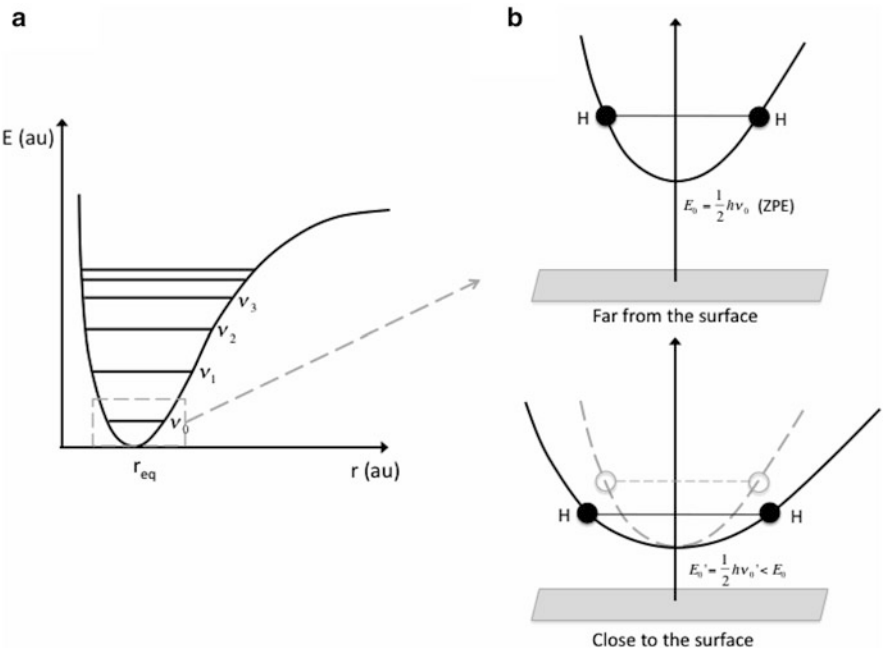

Fig. 2.1 Schematic representation of (**a**) vibrational states of a diatomic molecules and (**b**) vibrational softening

performed almost routinely for H_2 and its isotopes [32,53–55,57]. Full-dimensional quantum dynamics simulations based on coupled-channel (CC) and time-dependent wave packet (TDWP) methods have already been performed for reactive and nonreactive scattering of H_2 on low-index surfaces of various metals: Pd(100) [36, 38], Cu(100) [56], sulfur-precovered/Pd(100) [37], Pd(110) [15], Cu(111) [14,20], Cu(100) [86], Pt(111) [74], Pd(111) [7,8,18,29], Rh(111) [16], NiAl(110) [78], Cu(110) [58], CO-precovered/Ru(0001) [31], and c(2×2i)-Ti/Al(100) [9].

In order to test their theoretical models, the strategy used by surface scientists is to perform studies on benchmark systems for which experimental as well as theoretical analysis can be performed with similar accuracy. Throughout this chapter we will discuss six-dimensional quantum dynamics simulations performed on several of these H_2/metal surface benchmark systems, and we will analyze the results with the focus on the role played by the different DOFs. We will pay special attention to the effect that preexciting the vibrational DOFs has on molecular reactivity. As dissociative chemisorption involves stretching bonds until they rupture, reactivity of molecules on surfaces is closely related to energy transfer to and from the vibrational DOF. This energy transfer occurs not only for vibrationally excited molecules, where a deexcitation to the ground state causes an energy flux to the other DOFs. In fact, as we will discuss in the following section, the zero point energy (ZPE) of the molecule, the vibrational energy of the molecule ground state (see Fig. 2.1), can have a key effect on the reactivity of the so-called non-activated systems. In this case,

there can be an energy transfer from vibration to translation induced by vibrational softening. This vibrational softening occurs whenever a molecule approaches an attractive surface, and the attractive force between the surface and the atoms of the molecule becomes larger than the intramolecular force. This leads to a reduction of the force constant associated with the vibrational motion and, therefore, to the relaxation of the intramolecular bond. This bond relaxation induces a decrease in the potential well curvature, and, therefore, a decrease in the ZPE value (see Fig. 2.1).

We will also discuss first progress in the quantum dynamical treatment of polyatomic molecules (methane) reacting on surfaces, which has come possible, thanks to the development of reduced dimensionality models treating at least one vibrational mode of the molecule, and modeling the surface motion.

Finally, we should point out that quantum dynamics simulations represented throughout this chapter have been performed taking advantage of the Born–Oppenheimer approximation (BOA). In applying the BOA it is assumed that the interaction between the molecule and the surface takes place on the electronic ground state, i.e., that the electronic non-adiabatic effects are very small. Thus, these kind of studies are performed in two consecutive steps. First, the potential energy surface (PES), i.e., the electronic structure of the system, is computed, generally, using Density Functional Theory (DFT) [41, 51]. Quantum (and also classical) dynamics needs a continuous representation of the PES. Hence as an intermediate step the interpolation of the PES, for example with the corrugation reducing procedure [5], the modified Shepard method [13] or neural networks [62], is needed. Second, the motion of the nuclei on these PES is simulated. In this chapter, we will focus on this second step, the dynamics. At that point, we should also remark that most of the results presented here have been obtained by keeping the surface atoms fixed in the calculations, i.e., the energy transfer to and from phonons are neglected.

2.2 Reactive and Nonreactive Scattering of Molecules from Metal Surfaces

Molecule/surface systems are typically divided into two main groups, activated and non-activated systems. Activated systems are those in which the molecule needs a minimum energy to dissociate on the surface, i.e., those which present a minimum reaction barrier. On the other hand, systems with at least one barrierless reaction path are called non-activated. In the following, we show some representative quantum dynamics studies for prototypical activated and non-activated systems.

2.2.1 H_2/Metal Surfaces

2.2.1.1 Non-activated Systems

The first full-dimensional quantum dynamical calculations on dissociative adsorption were carried out on H_2/Pd(100) [38] (a non-activated system). These

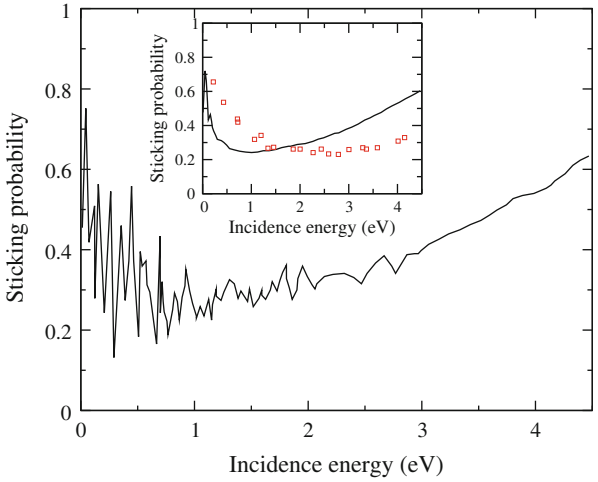

Fig. 2.2 Sticking probability versus incidence energy, under normal incidence, for $H_2(v = 0, J = 0)$/Pd(100) [38]. The *inset* show the convoluted sticking probability that account for the experimental molecular beam characteristics (*solid line*), and, for the sake of completeness, the experimental data from [75] (*square symbols*)

calculations showed a non-monotonous behavior of the dissociative adsorption (or sticking) probability as a function of the incidence energy of the molecule. This behavior was not unexpected for non-activated systems [75], but the sticking features are that the first it is not due to a precursor mechanism (see below) and second a strong oscillatory structure for low incidence energies (see Fig. 2.2), which, to present, has not been found experimentally. Before discussing the origin of these oscillations, it is worth mentioning that similar oscillations have been found later for other non-activated systems, such as H_2/Pd(110) [15], H_2/Pd(111) [7] and H_2/W(100) [49]. These oscillations have been attributed to the opening up of new diffraction and rotational excitation channels [35], which could explain why they are not obtained from classical (or quasiclassical) calculations, where neither the parallel momenta nor the energy take on discrete values, but change gradually. On the other hand, one may wonder why these oscillations are not observed experimentally. To answer this question we have to take into account the practical limitations of experimental setups. Whereas quantum calculations are performed considering a monoenergetic molecular beam containing H_2 in a well-defined quantum state (v,J) colliding with a frozen surface, the experimental molecular beams are not monochromatic, but display an energy spread, and the molecules are not only in the rovibrational ground state, but also occupy several rovibrational states according to a Boltzmann distribution. Furthermore, once the first impinging molecules are adsorbed, the perfect periodicity of the PES of the clean surface is destroyed. It should be also taken into account that the surface has a finite temperature, which reduces the coherence of the scattering process. And one should

also consider the influence of the incidence angle—usually >0 deg in experiments. All these factors smooth the experimental sticking curve. In fact, if the Boltzmann rovibrational distribution and the energy width of the experimental molecular beam are taken into account in the theoretical simulations, the quantum curve also shows a smooth appearance (see inset Fig. 2.2).

As shown in Fig. 2.2, quantum results on H_2/Pd(100) reproduce the initial decrease of the sticking probabilities observed experimentally in non-activated systems quite well. These results proved for the first time that this behavior is not due to any precursor state, as previously hypothesized, but to a purely dynamical mechanism. Initially it was suggested to be a pure steering mechanism, but later it was shown using classical trajectories that dynamics trapping contributes significantly to this behavior [6]. On the other hand, a comparison with quasi-classical dynamics simulations showed the key role played by the zero-point energy (ZPE) in the hydrogen dynamics [36]. Quasi-classical simulations suffer from the so-called violation of the ZPE: the initial ZPE can flow freely between all the molecular DOFs, which is not allowed in a quantum calculation. And as a result of this classical phenomenon the nonmonotonic behavior disappears in the quasi-classical results. The nonmonotonic behavior can be retrieved from classical calculations by leaving out the ZPE, i.e., by performing pure classical calculations, but in this case the sticking probability may be too low, because then the vibrational softening cannot be taken into account. It should be noted here that later it was shown that the parametrization of the PES used for the quantum dynamics simulations contained an artificial symmetry, which caused a lowering of the sticking probability [33]. However, all qualitative conclusions drawn from the quantum simulations [36, 38] still remain valid.

Thanks to the quantum dynamics simulations the role played by the internal degree of freedom of the molecule could also be analyzed, for both the rotational [24, 38] and the vibrational [34] mode. Quantum calculations have shown that molecular rotation suppresses the sticking of H_2 on Pd(100); the faster the molecules are rotating, the more the dissociative adsorption is suppressed. A closer inspection of these $J > 0$ results reveals that the suppression of sticking is due to molecules rotating in the so-called cartwheel rotation mode, $m_J = 0$. A similar result has been obtained for another non-activated system H_2/Rh(100) [24]. According to detailed balance, the consequence of these results, taken into account the principle of microscopic reversibility, is that the populations of rotational states in associative desorption is lower than expected for molecules in thermal equilibrium with the surface temperature (see Fig. 2.3). This rotational cooling was also found experimentally [81]. However, this behavior is not general for non-activated systems. Indeed, quantum calculations performed on H_2/Pd(110) [15] show a strong rotational enhancement in dissociative adsorption, which leads to rotational heating in associative desorption (see Fig. 2.3). In the case of Pd(111) [88] the scenario is even more complicated. At low incidence energy the dissociative adsorption probability first decreases with J and then increases, in agreement with experiments [30].

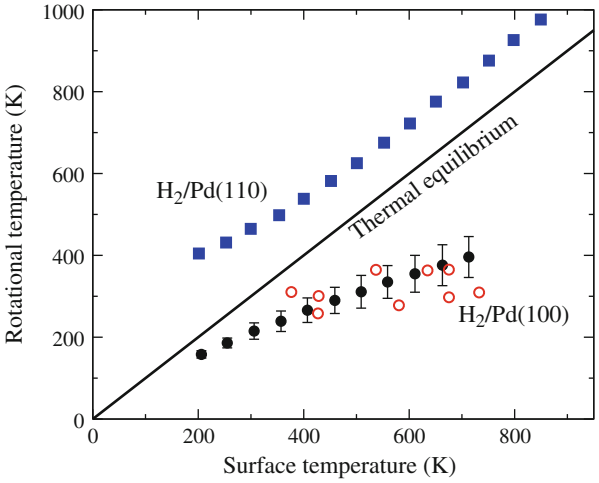

Fig. 2.3 Rotational temperatures of desorbing H_2 molecules from Pd(100): *solid black circles* theory from [38] and *red open circles* experiment from [81]. And from Pd(110): *solid blue squares* theory from [15]. The *solid line* corresponds to molecules in equilibrium with the surface temperature

As mentioned above, the suppression of sticking in H_2/Pd(100) by rotation is due to the cartwheel mode ($m_J = 0$), whereas the helicopter ($|m_J| = J$) mode enhances reactivity, i.e., quantum results suggest a strong steric effect. In order to verify this steric effect, the rotational quadrupole alignment parameter defined as:

$$A_0^{(2)}(J) = \left\langle \frac{3m_j^2 - J^2}{J^2} \right\rangle, \tag{2.1}$$

was computed from the fully initial-state resolved quantum sticking probabilities. $A_0^{(2)}(J)$ can change from -1 (molecules rotating in cartwheel fashion) to 2 (molecules rotating in helicopter fashion). In Fig. 2.1 the rotational alignment parameter as a function of the rotational quantum number, as obtained in [24], is shown. From this figure it can be seen that the $A_0^{(2)}(J)$ values are positive, and very similar to the experimental ones [90], confirming the steric effect. Results for H_2/Pd(110), shown in Fig. 2.4, show positive values [15], but much smaller than the ones computed for Pd(100).

The role of the initial vibrational state of the H_2 molecule has been also analyzed. This was done by means of the so-called vibrational efficacy, which gives a measure of the effectiveness of the vibrational energy to promote the dissociative adsorption. The vibrational efficacy can be computed using the simple formula:

$$\eta_v = \frac{E_0(v = 0, J = 0) - E_0(v = 1, J = 0)}{\hbar\omega_{\text{vib}}}, \tag{2.2}$$

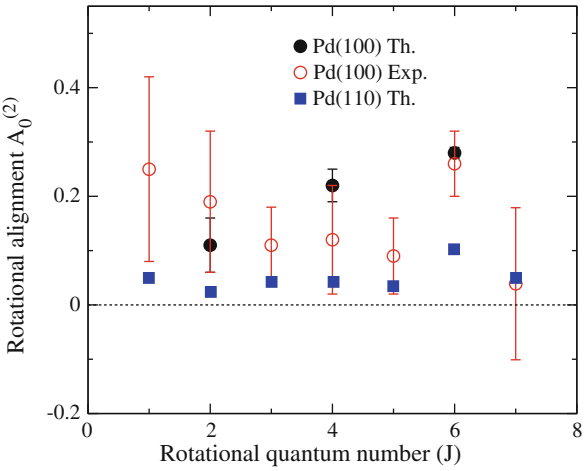

Fig. 2.4 Rotational quadrupole alignment parameter for desorbing H_2 molecules as a function of the rotational quantum number for a surface temperature $T = 700$ K. *Solid black circles*: theoretical results for Pd(100) from [24]. *Red open circles*: experimental results for Pd(100) from [90]. *Solid blue squares*: theoretical for Pd(110) from [15]

where E_0 is the translational energy required to obtain a dissociative adsorption probability S, so that η_v represents the separations of the sticking curves for a certain sticking probability divided by the gas-phase vibrational quantum $\hbar\omega_{\text{vib}} = 516$ meV. The value of η_v obtained for H_2/Pd(100), computed for $S = 0.7$, was 0.75, i.e., of the vibrational energy is 0.75 times as effective in promoting the dissociative adsorption as translational energy. This value is strikingly high compared with values obtained for other H_2/metal surface systems. Still higher values have been found for other molecules reacting on metal surfaces such as N_2 on Ru(0001) [17] and CH_4 on Ni(111) [85].

A detailed analysis allowed the mechanism behind the high effectiveness of vibration in promoting sticking to be revealed. Contrary to previous suggestions, this is not necessarily due to a strong curvature of the reaction path and to a late minimum reaction barrier to dissociative adsorption. It can also arise from a strong lowering of the molecular vibrational frequency during the adsorption and to the multi-dimensional character of the relevant phase space with its broad distribution of barrier heights [34]. At this point, it is worthy mentioning that this analysis could not be performed using classical simulations for the reasons discussed above.

Quantum dynamics simulations have also allowed the study of a purely quantum effect, molecular diffraction [18,22,29]. Molecular diffraction, observed experimentally for the first time in the 1930s [26], revealed the wave nature of the molecular motion. If we take into account the relationship between the de Broglie wavelength associated with the molecular beam, λ, and its wave vector, k, ($\lambda = 2\pi/k$) according to the Bragg condition for diffraction [27], molecular diffraction from a periodic surface occurs when the variation of the parallel wave vector **K** coincides

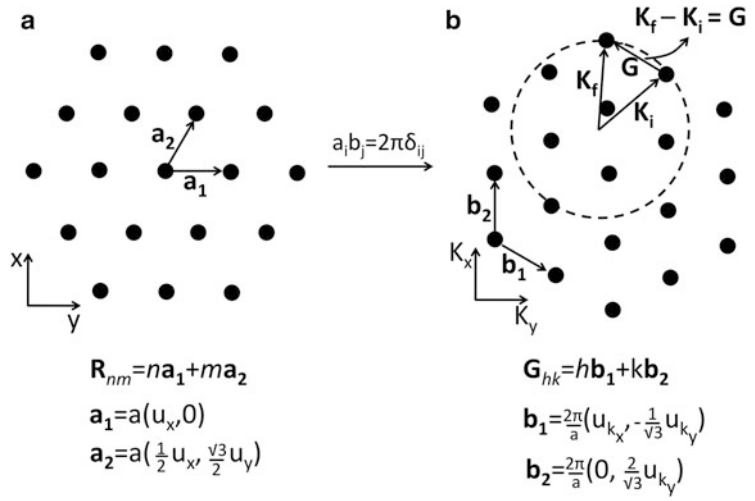

Fig. 2.5 (**a**) Schematic representation of a hexagonal real space. (**b**) Schematic representation of the corresponding reciprocal space and the Ewald sphere for diffraction

with a vector of the reciprocal lattice **G** (see Fig. 2.5). That is, diffraction occurs whenever

$$\mathbf{K}_i + \mathbf{G}_{n,m} = \mathbf{K}_f, \tag{2.3}$$

with $\mathbf{G}_{n,m} = n\mathbf{b}_1 + m\mathbf{b}_2$, where $\mathbf{b}_1$ and $\mathbf{b}_2$ are the basis vectors of the reciprocal lattice. For the sake of completeness, we point out that, taking into account the variation of the internal energy (rotational excitation and deexcitation), the molecular diffraction condition can be written as

$$k_{z,f}^2 = k_i^2 - \frac{4M\Delta E_{\text{rot}}}{\hbar^2} - (\mathbf{K}_i + \mathbf{G}_{n,m})^2 > 0. \tag{2.4}$$

where M being the mass of the molecule, $k_{z,f}$ the final perpendicular wave vector, k_i the initial total wave vector, and ΔE the change of the rotational energy. In the equation above, we have taken into account that, at the typical experimental impact energies, vibrational excitation is not possible.

Diffraction of molecules from metal surfaces has been widely studied experimentally for activated molecule/surface systems [27]. But, due to their complexity, only few 6D theoretical results are available in the literature. Here, we discuss the first 6D calculations on a non-activated system, H_2/Pd(111), published in 2004 [29]. Molecular diffraction from a non-activated system represents a challenge not only from a theoretical point of view, but also for experiments, because in this case most of the molecules dissociate on the surface, even for very low incidence energies. Therefore, in order to prevent the building-up of an adsorbed layer of hydrogen

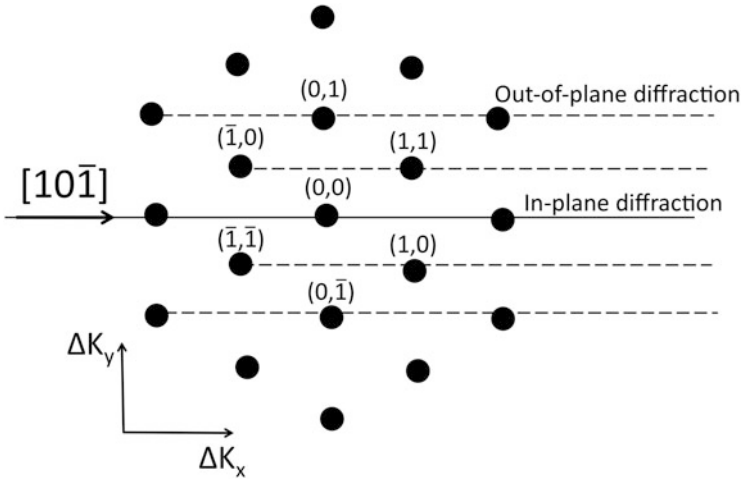

Fig. 2.6 Schematic representation of in-plane and out-of-plane diffraction

during the experiment, the surface temperature has to be kept at about 430 K, which enhances the surface atom vibrations, causing destructive inferences that quench diffraction. Furthermore, as these non-activated systems are very corrugated, inelastic diffraction is expected to dominate the spectra, increasing the number of diffraction peaks and decreasing their probabilities. These two phenomena explain why there were no attempts to measure diffraction in non-activated systems before 2004. But 6D quantum dynamics calculations, which suggested that the H_2/Pd(111) diffraction spectrum is dominated by first order out-of-plane diffraction peaks (see Fig. 2.6 for out-of-plane definition), stimulated the carrying out of diffraction experiments on this system. The experimental measurements corroborated theoretical results (see Fig. 2.7). Digging deeper into theoretical data, it was noticed that the out-of-plane peaks present in the spectra[2], associated with changes of K perpendicular to the incidence direction (parallel to the surface), were much larger than the peaks representing changes in the longitudinal direction. For example, if the incident molecular beam is aligned with the [10$\bar{1}$] direction (see Fig. 2.6), an out-of-plane diffraction peak observed in the spectrum is the (0,1) one (see Fig. 2.7): this peak is associated with $\Delta K_y = K_y$ and $\Delta K_x = 0$. It should be also noticed that in both experiments and theoretical simulations, the angle between the molecular beam incidence direction and the normal to the surface is quite high, $\theta_i = 50°$. Theoretical simulations considering low incidence angles did not show such transversal out-of-plane diffraction predominance. A complete analysis of the quantum theoretical simulations reveals that there is a direct relationship between the incidence angle

[2]Several initial conditions of the molecular beam were analyzed.

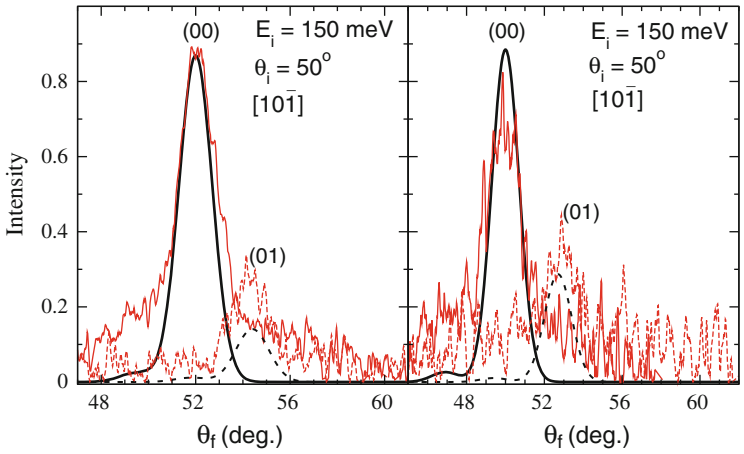

Fig. 2.7 Typical diffraction spectra for H_2/Pd(111). *Black line*: quantum results and *red line* experimental measurements; *solid line*: in-plane-diffraction; and *dashed line*: out-of-plane diffraction

and the transversal out-of-plane diffraction probability. This phenomenon is due to the periodicity of the potential[28]: the higher the incidence angles, the higher the periodicity of the potential felt by the molecules along the incidence direction, and in the extreme case of $\theta_i = 90°$ the molecule will feel a perfectly periodic potential and therefore along this direction $\Delta K = 0$, and, therefore, only changes of K in the perpendicular direction are possible.

Although this prominent out-of-plane diffraction has been observed for a non-activated system, it is a general phenomenon that is expected to be observed whenever the incidence angle is high enough, for example, prominent out-of-plane diffraction have been observed later on for H_2/Pt(111) [71] H_2/Ru(0001) [72] and H_2/Cu/Ru(0001) [22]. Furthermore, [28, 29] hypothesized that at grazing incidence and high incidence energy only out-of-plane transversal diffraction peaks could be observed. This hypothesis was confirmed experimentally a few years later [80, 82].

2.2.1.2 Activated Systems

Quantum dynamics on dissociative adsorption of the prototype activated system $H_2(D_2)$/Cu(111) have been essential, together with an accurate potential energy surface [21], to reproduce experimental observables with chemical accuracy [19].

As already mentioned in Sect. 2.2.1.1 to perform a meaningful comparison with experimental results, both the rovibrational distribution and the energy width of the molecular beam have been taken into account [20]. In order to do so, first the quantum monoenergetic state-resolved sticking probabilities, $S(v, J; E)$, are computed for a large range of incidence energies and the rovibrational states populated in molecular beams experiments. These probabilities are used to compute the

monoenergetic probabilities $S(T_n; E)$, which only depend on the incidence energy and on the nozzle temperature—this later one determines the rovibrational state distribution of the molecules in the molecular beam. $S(T_n; E)$ can be computed as:

$$S(T_n; E) = \sum_{v,J} F_{\mathrm{B}}(v, J; T_n) S(v, J; E), \tag{2.5}$$

where the Boltzmann factor, F_{B}, of each (v, J) state is given by:

$$F_{\mathrm{B}}(v, J; T_n) = (2J + 1) \exp[-E_{\mathrm{vib}}/kT_n] \times w(J) \exp[-E_{\mathrm{rot}}/0.8kT_n]/N, \tag{2.6}$$

where N is the normalization factor and $w(J)$ is the factor describing the nuclear spin statistics. From these computed monoenergetic reaction probabilities, molecular beam experimental results can be simulated by convolution over the distribution of the molecular beam, according to the expression:

$$S(T_n) = \frac{\int_{v=0}^{v=\infty} f(v; T_n) S(E, T_n) dv}{\int_{v=0}^{v=\infty} f(v; T_n)}, \tag{2.7}$$

where $E = \frac{1}{2} M v^2$, v being the velocity of the molecule and M its total mass. The flux weighted velocity distribution $f(v; T_n)$ is given by:

$$f(v; T_n) dv = C v^3 \exp[-(v - v_0)^2/\alpha^2] dv. \tag{2.8}$$

This latter equation includes the parameters describing the energy (or velocity) distribution of the molecular beam, the stream velocity v_0, and the width of the velocity distribution α, C being a constant.

Beyond simulating the experimental molecular beam characteristics, to be able to properly reproduce experimental results, an accurate PES has to be used [19]. At present, the only quantum electronic method able to treat the huge number of electrons involved in a molecule/surface system is DFT[3] (density functional theory), of which the accuracy depends on the accuracy of the exchange-correlation functional that was chosen. A sound strategy to choose the functional consists in fitting experimental results for one specific case to theoretical simulations based on PESs using different functionals, in an approach called the specific reaction parameter (SRP) approach to DFT [11]. An innovation applied to H_2/metal systems has been to take the SRP functional as a weighted average of GGA functionals [19]. In the study performed in [19] on $H_2(D_2)$/Cu(111), the functionals used were PW91 (Perdew–Wang 1991) [73] and RPBE (Revised Perdew–Burke–Ernzerhof) [39]. In this case, the specific experiment chosen was the dissociative

[3]The description of the method is beyond the scope of this chapter.

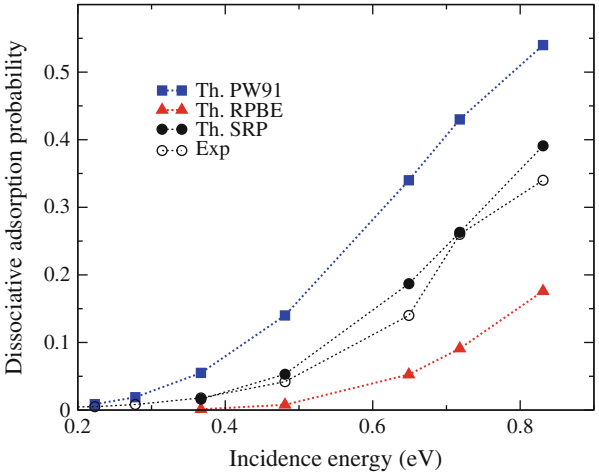

Fig. 2.8 Dissociative adsorption probabilities as a function of incidence energy for D_2/Cu(111), for a nozzle temperature T_n =2,100 K. Experimental data from [77]. Quasi-classical theoretical data from [19]

adsorption probability of D_2 for a nozzle temperature equal to 2,100 K, seeding in H_2 (see Fig. 2.8). The comparison between the theoretical and the experimental results showed that PW91-based theoretical results overestimated the experimental sticking probabilities, whereas the RPBE-based results underestimated them. Thus, none of these functionals yielded chemical accurate results, but a more accurate potential was obtained by combining these two functionals, using a specific reaction parameter (SRP) strategy, in such a way that the exchange-correlation part of the new functional is written as:

$$E_{\mathrm{xc}}^{\mathrm{SRP}} = xE_{\mathrm{xc}}^{\mathrm{PW91}} + (1-x)E_{\mathrm{xc}}^{\mathrm{RPBE}}, \tag{2.9}$$

where x being the mixing parameter chosen to accurately simulate the experimental results, as shown in Fig. 2.8.

This new SRP functional yielded chemically accurate (errors $\leq$1 kcal/mol $\approx$ 0.043 eV) results for a number of experimental observables. For example, in Fig. 2.9, dissociative adsorption probabilities as a function of the incidence energy, in comparison with experimental data, are shown for H_2/Cu(111). In this figure the theoretical results were obtained by using the SRP-PES and the corresponding parameters characteristic of each experimental molecular beam measurement. The theoretical results agree within chemical accuracy with the experimental ones. Furthermore, this study, published in 2009 [19], allowed to unravel a previous unsolved puzzle: why, at similar translational energies, did the two sets of experimental sticking probabilities, shown in Fig. 2.9, differ by an order of magnitude?

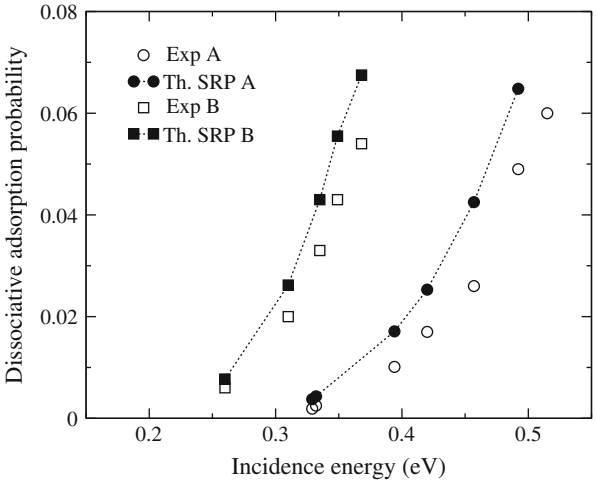

Fig. 2.9 Dissociative adsorption probabilities as a function of the incidence energy for a pure H_2 molecular beam on Cu(111). Experimental data A (*solid circles*) from [77]. Experimental data B (*solid squares*) from [3]. Theoretical data from [19]

The solution came from a detailed analysis of the molecular beam, which was needed to perform a meaningful comparison with theoretical simulations. The experimental sticking probabilities of [3] were larger because this group used molecular beams with wider energy distributions, the tails of which overlap to a greater extent with the portion of the energy-resolved reaction probability curve that steeply rises above threshold.

Quantum state-to-state scattering calculations also reproduced the rotationally inelastic scattering [19, 20] trend observed experimentally [40], according to which the rotationally inelastic scattering probability from $H_2(v = 1, J = 0)$ to $H_2(v = 1, J = 2)$ first increases with translational energy, E, reaching a maximum at around 0.14 eV, and then decreases when E increases. Quantum results show the same nonmonotonic behavior (see Fig. 2.10), but with the maximum at around 0.18 eV. As shown in Fig. 2.10 the theoretical data are shifted to higher values of E by about 0.039 eV, i.e., once again the agreement is within chemical accuracy. Additionally, quantum results showed that a further increase in the translational energy induces an increase of the rotational inelastic scattering probabilities.

A detailed comparison between experiments and quantum dynamics and AIMD (ab initio molecular dynamics) simulations has also been used to hypothesize about the prominent role that surface degrees of freedom (SDOFs) may have. For example, quantum vibrational excitation probabilities for H_2/Cu(111) and rotational alignment parameters for D_2/Cu(111) [20] do not show chemical accuracy, contrary to the case of the observables discussed above. However, these less accurate results could be attributed to a failure of the static surface approximation [59]. In Fig. 2.11

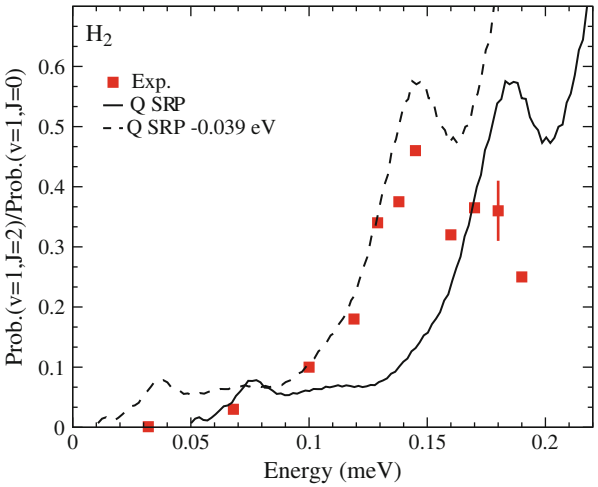

Fig. 2.10 Ratios of rotationally inelastic probabilities for $H_2(v = 1, J = 2)$ scattered from Cu(111). Experimental data from [40]. Theoretical data from [19]

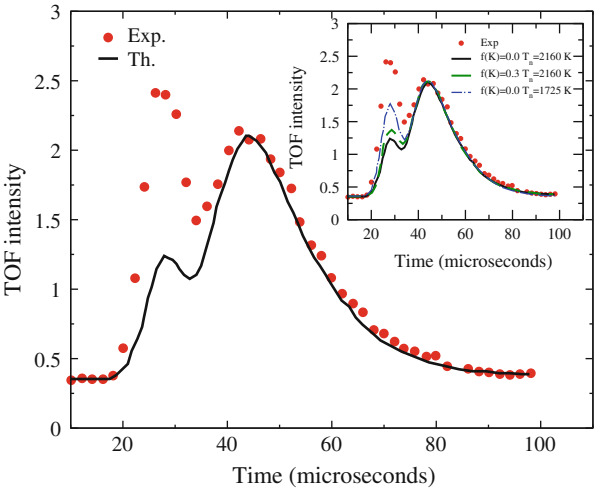

Fig. 2.11 TOF spectrum of H_2 scattered from Cu(111) into the state $(v = 1, J = 3)$. Experimental data, with T_s =400 k, from [76]. Theoretical data from [59] assuming total energy scaling. *Inset* also shows theoretical data as a function of the nozzle temperature, T_n, and as a function of the translational energy loss, $f(K)$

the experimental and theoretical time-of-flight (TOF) spectrum for $H_2(v, J \rightarrow v = 1, J = 3)$/Cu(111) are shown. In order to simulate theoretically the experimental TOF spectrum the expression

$$f(t,T_n) = c + N \times \left[\left(\frac{v_i}{v_0}\right)^4 \times \left[-\left(\frac{v_i - v_0}{\alpha}\right)^2\right] \times P(v = v', J = J' \rightarrow v', J')\right.$$
$$+x_t \times \left(\sum_{vJ,v'J' \neq} \left(\frac{v_i^3}{v_s v_0^4}\right) \times \left(\frac{1}{x_i v_i^{-2} + x_s v_i v_s^{-3}}\right) \times \exp\left[-\left(\frac{v_i - v_0}{\alpha}\right)^2\right]\right.$$
$$\left.\left.\times w_{vJ} \times P(v, J \rightarrow v'J')\right)\right] \tag{2.10}$$

was used. In this equation v_s represents the velocity of the scattered molecule, the parameter $x_i(x_s)$ describes the distance traveled by the molecule from the chopper (from the surface) to the surface (to the detecting laser), and w_{vJ} is the Boltzmann population of the initial (v, J) state in the incidence beams divided by the Boltzmann populations of the final (v', J') state in the incident beam, at the nozzle temperature used in the experiments.

From Fig. 2.11 it can be seen that there is a good agreement between the experimental and the theoretical *loss peak* exhibited by the spectra at long times. This *loss peak* reflects the loss of $H_2(v = 1, J = 3)$ due to dissociative adsorption, vibrational deexcitation, and rotational redistribution within $v = 1$. Thus, this excellent agreement showed that the Born–Oppenheimer static surface model provides an accurate simultaneous description of these processes. On the other hand, the *gain peak* at short times, due to vibrational excitation from $H_2(v = 0)$ to $H_2(v = 1, J = 3)$, is strongly underestimated by quantum simulations. The factors that may contribute to this disagreement between theoretical and experimental TOF spectrum have been discussed in [59]. The first one concerns the fraction of translational energy lost $(f(K))$ by H_2 and D_2 molecules scattered from Cu surfaces, estimated, from experimental measurements on vibrational deexcitation [89], to be of the order of 30 %. This energy loss is not taken into account in the static surface approximation. In fact, taking this phenomenon into account increases the agreement between theory and experiment, as shown in the inset of Fig. 2.11. A second factor is related to the uncertainties of the experimental nozzle temperature. As shown in the inset of Fig. 2.11 the intensity of the gain peak increases when T_n decreases. Eventually, the surface temperature (T_s) also plays a role in the vibrational excitation. A detailed analysis of experimental data on H_2 vibrational excitation as a function of the surface temperature [76] shows that increasing T_s from 400 to 700 K increases the contribution of vibrational excitation by about 20 %.

Rotational quadrupole alignment parameters $(A_0^{(2)})$ as a function of the translational energy represent another example of the role of the SDOFs. In Fig. 2.12 experimental and quantum simulated $A_0^{(2)}$ for D_2 as a function of the translations energy are shown. This figure shows the good agreement between experiments [42] and quantum theory [20]. But, this agreement is not within chemical accuracy as in the case of dissociative adsorption or vibrational deexcitation, despite the fact that the same accurate SRP-PES is used in all the cases. In order to explore the role played by the SDOFs, AIMD calculations [33] have shown themselves to be a very useful tool [68]. AIMD simulations, which include the SDOFs, yielded $A_0^{(2)}$ values

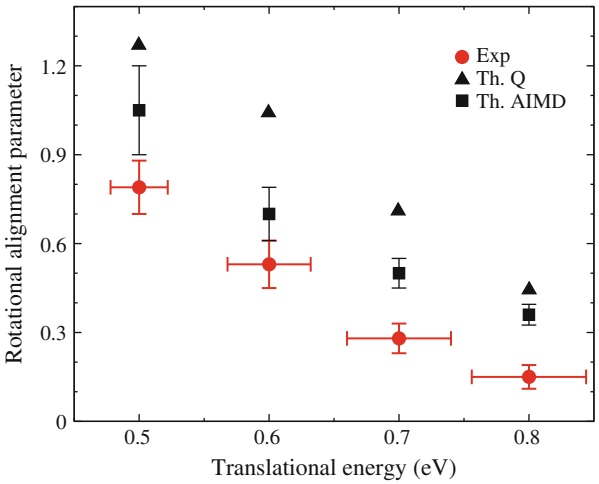

Fig. 2.12 Rotational alignment parameters as a function of the translational energy. Experimental data from [42]. Quantum dynamics data from [20]. AIMD data from [68]

in better agreement with experiments (see Fig. 2.12), showing the non-negligible role played by the surface motion in this physical process. In this case, quantum dynamics simulations results were used as reference data to evaluate the effect of surface motion.

Finally quantum dynamics simulations on dissociative adsorption and molecular diffraction for H_2/Pt(111) [74] allowed the solution of a long-standing experimental paradox regarding the corrugation of the system. On one hand, Luntz et al. [64] suggested a quite corrugated PES based on molecular beam experiments on sticking of D_2 and H_2, showing the dependence of the sticking on the initial momentum of the molecule parallel to the surface. On the other hand, experiments on rotationally inelastic diffraction for HD, carried out by Cowin et al. [12], which showed almost no diffraction, suggested a quite flat PES. Quantum calculations performed by Pijper et al. [74] show that, in fact, increasing the initial parallel energy of the H_2 molecule inhibits reaction for low normal energy (see Fig. 2.13). This phenomenon has been explained in terms of the barrier heights encountered by the molecule. Due to the parallel momentum, the incident molecule samples barriers across the whole unit cell. Thus, increasing the parallel momentum increases the probability that the incident molecule encounters a higher barrier, leading to a decrease in reactivity.

An analysis of the complementary channel, molecular scattering, in terms of diffraction probabilities (see Fig. 2.14) reveals that the most populated first order diffraction peaks are not in-plane, but out-of-plane, (01) and $(0\bar{1})$ (see Fig. 2.6), which explains the very low diffraction probability found experimentally [12]. These experiments considered only for in-plane diffraction.

Later in [71], a detailed comparison, i.e., taking into account the rovibrational distribution of the molecular beam, with experiment, measuring both in-plane and

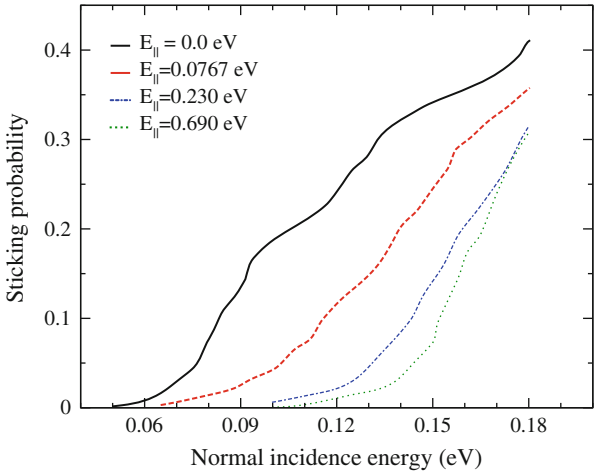

Fig. 2.13 Quantum reaction probabilities, for $H_2(v = 0, J = 0)$/Pt(111), for off-normal incidence as a function of the normal incidence energy. Results are for the rovibrational ground state ($v = 0, J = 0$), for incidence along the $[10\bar{1}]$ direction, and four different initial parallel energies

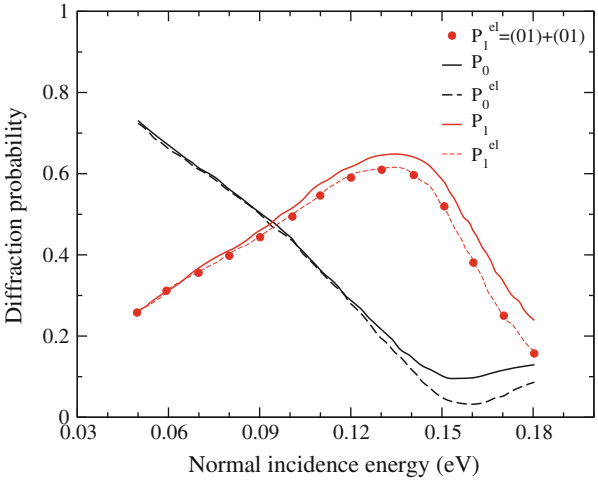

Fig. 2.14 Quantum diffraction probabilities versus normal incidence energy, for $H_2(v = 0, J = 0)$/Pt(111), for the zeroth and the first diffraction order, P_0 and P_1, along the incidence direction $[10\bar{1}]$. Rotationally elastic diffraction probability into the zeroth and first order, P_0^{el} and P_1^{el}, is also shown. $\tilde{P}_1^{el}$ refers to the part of P_0^{el} due to diffraction into the (01) and $(0\bar{1})$ out-of-plane diffraction peaks. These results correspond to $E_n = 0.69$ eV

out-of-plane diffraction, corroborated the importance of out-of-plane diffraction in the scattering of H_2 from Pt(111) (see Fig. 2.15). Furthermore, the good agreement obtained between quantum results and experiments, for both dissociative adsorption

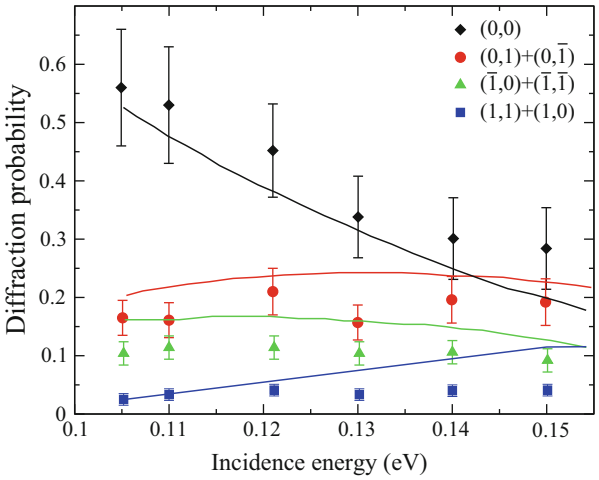

Fig. 2.15 Diffraction peaks probabilities versus incidence energy, for incidence along the $[10\bar{1}]$ direction. The experimental results are shown with *symbols*; the theoretical results are shown with *solid lines*

and scattering, has been considered a proof of the high accuracy of the Born–Oppenheimer approximation for H_2/metal systems.

2.2.2 CH_4/Metal Surfaces

Quantum dynamics calculations have also been performed on more complex systems, such as CH_4/metal surfaces. In fact, from an experimental point of view, the dissociation of methane on metals is one of the most studied reactions in surface science [2, 47, 60, 66, 85] because of its industrial relevance.

To simulate the reactivity of methane on metal surfaces a quantum treatment is preferred because the high barriers present on the PES lead to low reaction probabilities at lower energies, where tunneling is important. This is a real challenge for theoretical studies, given the large number of molecular DOFs. But this is not the only problem that theoretical studies have to face. At the high collision energies required for reaction, the interaction between the molecule and the atoms of the metal lattice is strong, and lattice motion has to be included in the calculation. Quantum dynamics calculations for dissociation of CH_4 on Ni(111) were performed by Jackson and others [69] using a reduced dimensionality scheme, where only one of the H-CH_3 bonds, the distance between the molecular center of mass and surface, and the rotation of the molecule, are considered. But, in addition to these molecule DOFs, the lattice motion was modeled by allowing the Ni atom over which the reaction occurs to move normal to the surface (Q). Dissociative adsorption probabilities obtained using this lattice relaxation (LR) model are shown in Fig. 2.16. The LR results shown in this figure, obtained by Boltzmann averaging

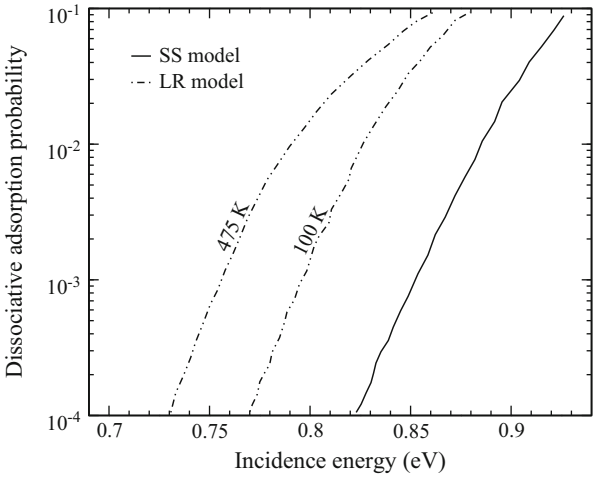

Fig. 2.16 Quantum dissociative adsorption probabilities as a function of translational energy for CH_4/Ni(111), for the molecular vibrational ground state. *Solid line*: SS model; *dot-dashed line*: LR model. For the later case two surface temperatures are shown, 100 and 475 K

over many lattice vibrational modes, are representative of the main results obtained in that study: (1) the LR model yielded higher reactivity than the static surface (SS) model; (2) the effects of lattice motion and relaxation on reactivity are strong at low translational energies where tunneling dominates. In spite of the approximations made in the LR model, the results were found to be in reasonable agreement with experiments. For example, the reactivity measured by Utz and others [85] for CH_4 in its vibrational ground state for $T_s = 475\,\text{K}$ and $E = 0.75\,\text{eV}$ is equal to 10^{-4}. The LR model gives the same reactivity at 0.73 eV.

Subsequent studies of CH_4 dissociation on Ni(111) [87], using both a mixed quantum/classical approach and the fully quantum model described above, showed that the motion of the lattice is relatively unperturbed by the incident molecule. In fact, Jackson and others [87] showed that a sudden treatment of the lattice motion reproduced fairly well the full-dimensional quantum results (see Fig. 2.17), but with a much lower computational effort. These studies also showed that the reactivity is dominated by collisions with metal atoms that are puckered out of the plane of the surface at the time of impact, as the barrier to methane dissociation is lower for these lattice configurations.

Without any doubt, the most striking results of the dissociative adsorption measurements of CH_4 on Nickel is the significant enhancement of reactivity for vibrationally excited molecules. For example, for CH_4/Ni(100), experiment [47,66] reveals that the ν_1 vibrational state (see Fig. 2.18) has the largest efficacy (η_ν) for promoting reaction. To analyze this observed behavior, and to shed some light on the physical mechanisms behind these observations, full-dimensional quantum simulations were performed [44, 70]. To carry out these simulations the Reaction

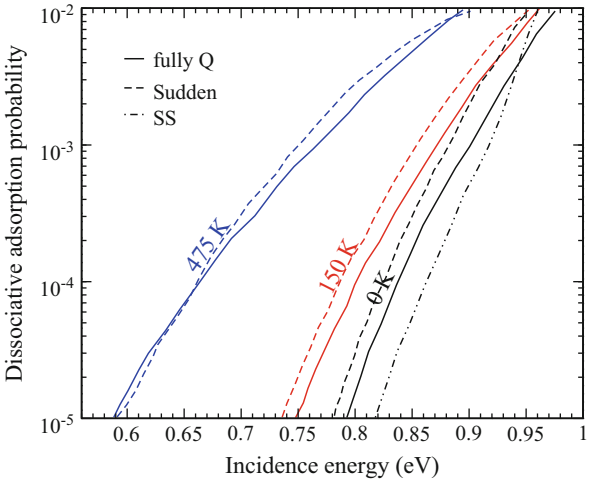

Fig. 2.17 Quantum dissociative adsorption probabilities as a function of the incidence energy for CH_4/Ni(111), for the molecular vibrational ground state. *Solid line*: fully quantum calculations; *dashed line*: sudden approximations; *dot-dashed line*: surface static approximations. Three surface temperatures are shown: 0, 100, and 475 K

Path Hamiltonian (RPH) [65,67] was used, including all 15 molecular DOFs within the harmonic approximation. In order to allow the evolution of the system and observe the possible transitions between different vibrational states, due to the non-adiabatic coupling that arises from the interaction between the molecule and surface, the total wavefunction was expanded in the adiabatic vibrational states of the molecule. Close-coupled equations were derived for wave packets propagating on a vibrationally adiabatic potential energy surfaces, with vibrationally non-adiabatic couplings linking these states to each other. In spite of the approximations made in deriving this quantum model, the theoretical results for the full-dimensional finite temperature dissociative adsorption probability are in very good agreement with experiments (see Fig. 2.19). As also shown in Table 2.1 the larger efficacy of the ν_1 state relative to the ν_3 state is reproduced.

A detailed analysis of the quantum results revealed the origin of this behavior. The increased efficacy of the ν_1 state arises from both mode softening and vibrationally non-adiabatic couplings. Furthermore this analysis revealed that most of the reactivity at the experimental surface temperature (475 K) is due to thermally assisted over-the-barrier processes, and not to tunneling. Tunneling becomes important at lower incidence energies and lower surface temperatures.

Low-dimensional quantum dynamics studies of the dissociative adsorption of CH_4 on Ni(111), as a function of the vibrational initial state, have also been carried out [52]. In this case, quantum dynamics simulations were performed using the multiconfiguration time-dependent Hartree (MCTDH) method [1]. Results obtained from this study are similar to those obtained for Ni(100): the efficacies of the stretching modes are larger than those of the bending modes, also in good agreement with experiments.

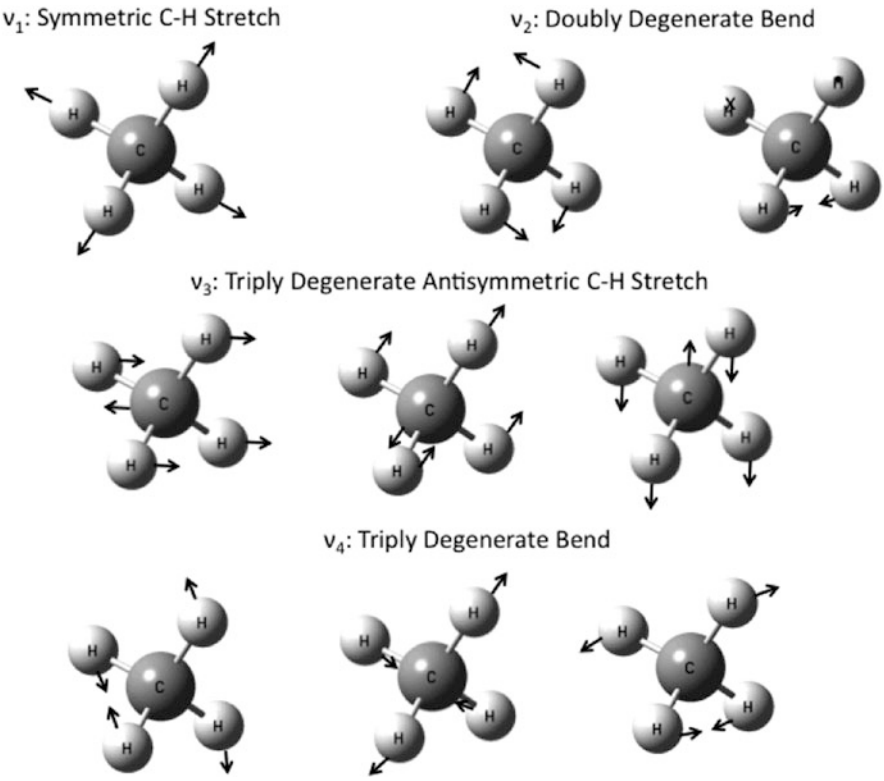

Fig. 2.18 Methane vibrational normal modes

2.3 Conclusions and Outlook

Throughout this chapter we have shown that quantum dynamics simulation on molecule/metal surface interactions have allowed the description of a significant number of physical phenomena related to both the molecular and the surface DOFs. In the case of the molecular DOF their role is investigated directly through quantum calculations, whereas the surface DOF has been investigated indirectly by using quantum data as reference ones. We have shown that nowadays state-of-the-art quantum simulations allow one to treat, fully quantum mechanically, light diatomic molecules (H_2, D_2 and HD) interacting with metal surfaces including the six DOFs of the molecule. Beyond these simple molecules, quantum dynamics simulations have been used to study the reactivity of methane on Ni surfaces, including only the relevant molecular DOFs. But, in spite of the reduce dimensionality of the simulations, they have allowed the identification of the physical mechanisms behind the observed experimental measurements.

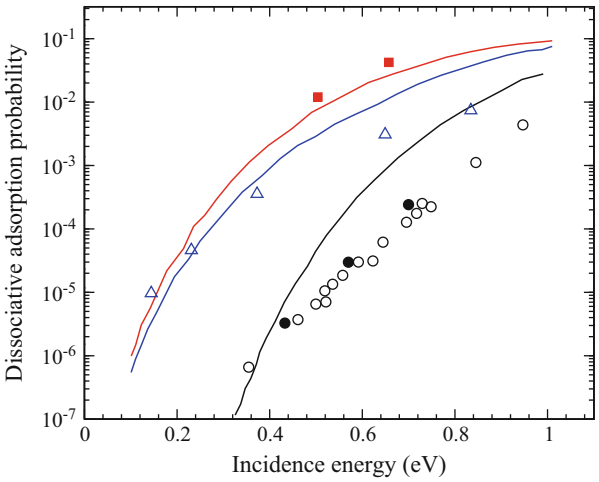

Fig. 2.19 Dissociative adsorption probabilities as a function of the incidence energy for CH_4/Ni(100), for several vibrational states. Theory from [44], *black line* for ν_0, *red line* for ν_1 and *blue line* for ν_3. *Black solid circles*: experimental data for ν_0 from [2]; *red solid squares*: experimental data for ν_1 from [2]; *black open circles*: experimental data for ν_0 from [46]; *blue open triangles*: experimental data for ν_3 from [46]

Table 2.1 Vibrational efficacies for CH_4/Ni(100)

Mode	η_{exp}	η_{th}
ν_1	1.4	0.93
ν_3	0.94	0.80

Experimental modes ν_1 and ν_3 taken from [47] and [46]. Theoretical data from [70]

In spite of the notable success of quantum dynamics achieved with describing molecule/surface interactions during the last few decades, surface scientists will have to face important challenges in the next future. Although at present state-of-the-art quantum dynamics simulations allow one to treat diatomic molecules with essentially no approximations relative to the molecular DOFs, still some effects cannot be included accurately. In this respect, the greatest challenge facing theorists in the field is to come up with a model that can yield accurate predictions for molecule–metal surface reactions involving excited electronic states with potential curve crossings [54]. These electronic excitations have been suggested, based on experimental measurements, to play a key role in phenomena such as vibrational quenching in associative desorption of N_2 from Ru(0001) [23] or multi-quantum vibrational relaxation of NO scattering from metal surfaces [43]. Till present day, several models have been developed to take into account non-adiabatic effects, with moderate success [45,63,83]. But a complete accurate description is most desirable. Time-dependent Density Functional Theory (TDDFT) [61] and embedding schemes involving high-level ab initio methods and DFT [50] may be of help. Also relative

to diatomic/molecule surfaces, an accurate description of the surface motion would be necessary.

Full dimensional quantum dynamics calculations on polyatomic molecules will hopefully lead to a deeper understanding on molecule/surface interactions mechanisms, as the six-dimensional quantum dynamics calculations have already done for H_2/metal surfaces. These kind of simulations are required to describe accurately processes involving the breaking of a X-R bond, beyond dissociation of CH_4 on H and CH_3. A description along the lines of the MCTDH (multi-configurational time-dependent Hartree) method would be worth exploring. For these polyatomic molecules, a better description of the molecule–lattice coupling is also desirable.

Acknowledgements C. Díaz acknowledges support under MICINN project FIS2010-25127.

References

1. Beck MH, Jäckle A, Worth GA, Meyer HD (2000) The multiconfiguration time-dependent Hartree (MCTDH) method: a highly efficient algorithm for propagating wavepackets. Phys Rep 324:1
2. Beck RD, Maroni P, Papageorgopoulos DC, Dang TT, Schmid MP, Rizzo TR (2003) Vibrational mode-specific reaction of methane on a nickel surface. Science 302:98
3. Berger HF, Leisch M, Winkler A, Rendulic KD (1990) A search for vibrational contributions to the activated adsorption of H_2 on copper. Chem Phys Lett 175:425
4. Besenbacher F, Chorkendorff I, Clausen BS, Hammer B, Malenbroek AM, Norskov JK, Stensgaard I (1998) Design of a surface alloy catalyst for steam reforming. Science 279:1913
5. Busnengo HF, Salin A, Dong W (2000) Representation of the 6D potential energy surface for a diatomic molecule near a solid surface. J Chem Phys 112:7641
6. Busnengo HF, Crespos C, Dong W, Rayez JC, Salin A (2002) Classical dynamics of dissociative adsorption for a nonactivated system: The role of zero point energy. J Chem Phys 116:9005
7. Busnengo HF, Pijper E, Somers MF, Kroes GJ, Salin A, Olsen RA, Lemoine D, Dong W (2002) Six-dimensional quantum and classical dynamics study of $H_2(v = 0,J = 0)$ scattering from Pd(111). Chem Phys Lett 356:515
8. Busnengo HF, Pijper E, Kroes GJ, Salin A (2003) Rotational effects in dissociation of H_2 on Pd(111): Quantum and classical study. J Chem Phys 119:12553
9. Chen JC, Juanes-Marcos JC, Woittequand S, Somers MF, Díaz C, Olsen RA, Kroes GJ (2011) Six-dimensional quasiclassical and quantum dynamics of H_2 dissociation on the c(2×2)-Ti/Al(100) surface. J Chem Phys 134:114708
10. Chorkendorff I, Niemantsverdriet JW (2003) Concepts of modern catalysis and kinetics. Wiley-VCH, Weinheim
11. Chuang YY, Radhakrisnan ML, Fast PL, Cramer CJ, Truhlar DG (1999) Direct dynamics for free radical kinetics in solution: solvent effect on the rate constant for the methanol with atomic hydrogen. J Phys Chem A 103:4893
12. Cowin JP, Yu CF, Sibener SJ, Wharton L (1983) HD scattering from Pt(111): Rotational excitation probabilities. J Chem Phys 79:3537
13. Crespos C, Collins MA, Pijper E, Kroes GJ (2004) Application of the modified Shepard interpolation method to the determination of the potential energy surface for a molecule-surface reaction:H_2+ Pt(111). J Chem Phys 120:2392
14. Dai J, Light JC (1997) Six dimensional quantum dynamics study for dissociative adsorption of H_2 on Cu(111) surface. J Chem Phys 107:1676

15. Dianat A, Gross A (2004) High-dimensional quantum dynamical study of the dissociation of H_2 on Pd(110). J Chem Phys 120:5339
16. Dianat A, Sakong S, Gross A (2005) Quantum dynamics of the dissociation of H_2 on Rh(111). Eur Phys J B 45:425
17. Díaz C, Olsen RA (2009) A note on the vibrational efficacy in molecule-surface reactions. J Phys Chem 130:094706
18. Díaz C, Somers MF, Kroes GJ, Busnengo HF, Salin A, Martín F (2005) Quantum and classical dynamics of H_2 scattering from Pd(111) at off-normal incidence. Phys Rev B 72:035401
19. Díaz C, Pijper E, Olsen RA, Busnengo HF, Auerbach DJ, Kroes GJ (2009) Science 326:832
20. Díaz C, Olsen RA, Auerbach DJ, Kroes GJ (2010) Six-dimensional dynamics study of reactive and non reactive scattering of H_2 from Cu(111) using a chemically accurate potential energy surface. Phys Chem Chem Phys 12:6499
21. Díaz C, Olsen RA, Busnengo HF, Kroes GJ (2010) Dynamics on six-dimensional potential energy surfaces for H_2/Cu(111): Corrugation reducing procedure versus modified Shepard interpolation method and PW91 versus RPBE. J Phys Chem C 114:11192
22. Díaz C, Martín F, Kroes GJ, Minniti M, Farías D, Miranda R (2012) H_2 diffraction from a strained pseudomorphic monolayer of Cu deposited on Ru(0001) J Phys Chem C 116:13671
23. Diekhöner L, Honekaer L, Mortensen H, Jensen E, Baurichter A, Petrunin VV, Luntz AC (2002) Indirect evidence for strong nonadiabatic coupling in N_2 associative desorption from and dissociative adsorption on Ru(0001). J Chem Phys 117:5018
24. Eichler A, Hafner J, Gross A, Scheffler M (1999) Rotational effects in the dissociation of H_2 on metal surfaces studies by ab initio quantum-dynamics calculations. Chem Phys Lett 311:1
25. Ertl G (1983) Primary steps in catalytic synthesis of ammonia. J Vac Sci Technol A 1:1247
26. Estermann I, Stern O (1930) Z Phys 63:95
27. Farías D, Rieder KH (1998) Atomic beam diffraction from solid surfaces. Rep Prog Phys 61:1575
28. Farías D, Díaz C, Nieto P, Salin A, Martín F (2004) Pronounced out-of-plane diffraction of H_2 molecules from a Pd(111) surface. Chem Phys Lett 390:250
29. Farías D, Díaz C, Rivière P, Busnengo HF, Nieto P, Somers MF, Kroes GJ, Salin A, Martín F (2004) In-plane and out-plane diffraction of H_2 from metal surfaces. Phys Rev Lett 93:246104
30. Gostein HG, Sitz GO (1997) Rotational state-resolved sticking coefficients for H_2 on Pd(111): Testing dynamical steering in dissociative adsorption. J Chem Phys 106:7378
31. Groot IMN, Juanes-Marcos JC, Díaz C, Somers MF (2010) Dynamics of dissociative adsorption of hydrogen on CO-precovered Ru(0001) surface: a comparison of theoretical and experimental results. R. A. Olsen and G. J. Kroes, Phys Chem Chem Phys 12:1331
32. Gross A (1998) Reactions at surfaces studied by ab initio dynamics calculations. Surf Sci Rep 32:291
33. Gross A, Dianat A (2007) Hydrogen dissociation dynamics on precovered Pd surfaces: Langmuir is still right. Phys Rev Lett 98:206107
34. Gross A, Scheffler M (1996) Influence of molecular vibrations on dissociative adsorption. Chem Phys Lett 256:417
35. Gross A, Scheffler M (1996) Scattering of hydrogen molecules from a reactive surface: Strong off-specular and rotationally inelastic diffraction. Chem Phys Lett 263:567
36. Gross A, Scheffler M (1998) Ab initio quantum and molecular dynamics of the dissociative adsorption of hydrogen on Pd(100). Phys Rev B 57:2493
37. Gross A, Scheffler M (2000) Dynamics of hydrogen dissociation at the sulfur-covered Pd(100) surface. Phys Rev B 61:8425
38. Gross A, Wilke S, Scheffler M (1995) Six-dimensional quantum dynamics of adsorption and desorption of H_2 at Pd(100): steering ans steric effects. Phys Rev Lett 75:2718
39. Hammer B, Hansen LB, Norskov JK (1999) Improved adsorption energetics within density-functional theory using revised Perdew-Burke-Ernzerhof functionals. Phys Rev B 59:7413
40. Hodgson A, Samson P, Wight A, Cottrell C (1997) Rotational excitation and vibrational relaxation of $H_2(\nu = 0, J = 0)$ scattered from Cu(111). Phys Rev Lett 78:963
41. Hohenberg P, Kohn W (1964) Inhomogeneous electron. Gas Phys Rev 136:B864

42. Hou H, Gulding SJ, Rettner CT, Wodtke AM, Auerbach DJ (1997) The stereodynamics of a gas-surface reaction. Science 277:80
43. Huang Y, Rettner CT, Auerbach DJ, Wodtke AM (2000) Vibrational promotion of electron transfer. Science 290:111
44. Jackson B, Nave S (2011) The dissociative chemisorption of methane on Ni(100): Reaction path description of mode-selective chemistry. J Chem Phys 135:114701
45. Juaristi JI, Alducin M, Díez-Muiño R, Busnengo HF, Salin A (2008) Role of electron-hole pair excitations in the dissociative adsorption of diatomic molecules on metal surfaces. Phys Rev Lett 100:116102
46. Juurlink LBF, McCabe PR, Smith RR, DiCologero CL, Utz AL (1999) Eigenstate-resolved studies of gas-surface reactivity: $CH_4(\nu_3)$ dissociation on Ni(100). Phys Rev Lett 83:868
47. Juurlink LBF, Smith RR, Killelea DR, Utz AL (2005) Comparative study of C-H stretch and bend vibrations in methane activation on Ni(100) and Ni(111). Phys Rev Lett 94:208303
48. Juurlink LBF, Killelea DR, Utz AL (2009) State-resolved probes of methane dissociation dynamics. Prog Surf Sci 84:69
49. Kay M, Darling GR, Holloway S, White JA, Bird DM (1995) Steering effects in non-activated adsorption. Chem Phys Lett 245:311
50. Klüner T, Govind N, Wang YA, Carter EA (2002) Periodic density functional embedding theory for complete active space self-consistent field and configuration interaction calculations: ground and excited states. J Chem Phys 116:42
51. Kohn W, Sham LJ (1965) Self-consistent equations including exchange and correlation effects. Phys Rev 140:A1133
52. Krishnamohan GP, Olsen RA, Kroes GJ, Gatti F, Woittequand S (2010) Quantum dynamics of dissociative chemisorption of CH_4 on Ni(111): Influence of the bending vibration J Chem Phys 133:144308
53. Kroes GJ (1999) Six-dimensional quantum dynamics of dissociative chemisorption of H_2 on metal surfaces. Prog Surf Sci 60:1
54. Kroes GJ (2008) Frontiers in surface scattering simulations. Science 321:794
55. Kroes GJ, Somers MF (2005) Six-dimensional dynamics of dissociative chemisorption of H_2 on metal surfaces. J Theor Comput Chem 4:493
56. Kroes GJ, Baerends EJ, Mowrey RC (1997) Six-dimensional quantum dynamics of dissociative chemisorption of ($v = 0$,$J = 0$) H_2 on Cu(100). Phys Rev Lett 78:3583
57. Kroes GJ, Gross A, Baerends EJ, Scheffler M, McCormack DA (2002) Quantum theory of dissociative chemisorption on metal surfaces. Acc Chem Res 35:193
58. Kroes GJ, Pijper E, Salin A (2007) Dissociative chemisorption of H_2 on the Cu(110) surface: A quantum and quasiclassical dynamical study. J Chem Phys 127:164722
59. Kroes GJ, Díaz C, Pijper E, Olsen RA, Auerbach DJ (2010) Apparent failure of the Born-Oppenheimer static surface model for vibrational excitation of molecular hydrogen on copper. PNAS 107:20881
60. Larsen JH, Chorkendorff I (1999) From fundamental studies of reactivity on single crystals to the design of catalysts. Surf Sci Rep 35:163
61. Lindenblatt M, Pehlke E (2006) Ab initio simulation of the spin transition during chemisorption: H/Al(111). Phys Rev Lett 97:216101
62. Lorenz S, Gross A, Scheffler M (2004) Representing high-dimensional potential-energy surfaces for reactions at surfaces by neural networks. Chem Phys Lett 395:210
63. Luntz AC, Persson M (2005) How adiabatic is activated adsorption/associative desorption? J Chem Phys 123:074704
64. Luntz AC, Brown JK, Williams MD (1990) Molecular beam studies of H_2 and D_2 dissociative chemisorption on Pt(111). J Chem Phys 93:5240
65. Marcus RA (1966) On the analytical mechanics of chemical reactions. Classical mechanics of linear collisions. J Chem Phys 45:4500
66. Maroni P, Papageorgopoulos DC, Sacchi M, Dang TT, Beck RD, Rizzo TR (2005) State-resolved gas-surface reactivity of methane in the symmetric C-H stretch vibration on Ni(100). Phys Rev Lett 94:246104

67. Miller WH, Handy NC, Adams JE (1980) Reaction path Hamiltonian for polyatomic molecules. J Chem Phys 72:99
68. Nattino F, Díaz C, Jackson B, Kroes GJ (2012) Effect of surface motion on the rotational quadrupole alignment parameter of D_2 reacting on Cu(111). Phys Rev Lett 108:236104
69. Nave S, Jackson B (2007) Methane dissociation on Ni(111): The role of lattice reconstruction. Phys Rev Lett 98:173003
70. Nave S, Jackson B (2010) Vibrational mode-selective chemistry: Methane dissociation on Ni(100). Phys Rev B 81:233408
71. Nieto P, Pijper E, Barredo D, Laurent G, Olsen RA, Baerends EJ, Kroes GJ, Farías D (2006) Reactive ans nonreactive scattering of H_2 from a metal surface is electronically adiabatic. Science 312:86
72. Nieto P, Farías D, Miranda R, Luppi M, Baerends EJ, Somers MF, van der Niet MJTC, Olsen RA, Kroes GJ (2011) Diffractive and reactive scattering of H_2 from Ru(0001): experimental and theoretical study. Phys Chem Chem Phys 13:8583
73. Perdew JP, Chevary JA, Vosko SH, Jackson KA, Pederson MR, Singh DJ, Fiolhais C (1992) Atoms, molecules, solids, and surfaces: applications of the generalized gradient approximation for exchange ans correlation. Phys Rev B 46:6671
74. Pijper E, Kroes GJ, Olsen RA, Baerends EJ (2002) Reactive and diffractive scattering of H_2 from Pt(111) studied using a six-dimensional wave packet method. J Chem Phys 117:5885
75. Rendulic KD, Anger G, Winkler A (1989) Wide range nozzle beam adsorption data for the system H_2/nickel and H_2/Pd(100). Surf Sci 208:404
76. Rettner C, Michelsen HA, Auerbach DJ (1993) Determination of quantum-state-specific gas-surface energy transfer and adsorption probabilities as a function of kinetic energy. Chem Phys 175:157
77. Rettner C, Michelsen HA, Auerbach DJ (1995) Quantum-state-specific dynamics of the dissociative adsorption and associative desorption of H_2 at a Cu(111) surface. J Chem Phys 102:4625
78. Rivière P, Somers MF, Kroes GJ, Martín F (2006) Quantum dynamical study of the H_2 and D_2 dissociative adsorption and diffraction from the NiAl(110) alloy surface. Phys Rev B 73:205417
79. Rostrup-Nielsen JR (1984) Catalysis: science technology. In: Boudart M, Anderson JR (eds). Springer, Berlin
80. Rousseau P, Khemliche H, Borisov AG, Roncin P (2007) Quantum scattering of fast atoms and molecules on surfaces. Phys Rev Lett 98:016104
81. Schröter L, David R, Zacharias H (1991) Rotational state distribution of recombinatively desorbing hydrogen from clean ans S-covered Pd(100). Surf Sci 258:259; Laser spectroscopy of hydrogen desorption from Pd(100). J Vac Sci Technol A 9:1712 (1991)
82. Schüller A, Wethekam S, Winter H (2007) Diffraction of fast atomic projectiles during grazing scattering from a LiF(001) surface. Phys Rev Lett 98:016103
83. Shenvi N, Roy S, Tully JC (2009) Dynamical steering ans electronic excitation in NO scattering from a gold surface. Science 326:829
84. Sinfelt JH (1979) Structure of metal catalysts. Rev Mod Phys 51:569
85. Smith RR, Killelea DR, DelSesto DF, Utz AL (2004) Preference for vibrational over translational energy in a gas-surface reaction. Science 304:992
86. Somers MF, McCormack DA, Kroes GJ, Olsen RA, Baerends EJ, Mowrey RC (2002) Signatures of site-specific reaction of H_2 on Cu(100). J Chem Phys 117:6673
87. Tiwari AK, Nave S, Jackson B (2009) Methane dissociation on Ni(111): a new understanding of the lattice effect. Phys Rev Lett 103:253201
88. van Willingen RT, Somers MF, Busnengo HF, Kroes GJ (2004) The dependence of dissociative chemisorption of H_2 on Pd(111) on H_2 rotation: a six-dimensional quantum dynamics study. Chem Phys Lett 393:166

89. Watts E, Sitz GO (2001) State-to-state scattering in a reactive system $H_2(\nu = 1,J = 1)$ from Cu(100). J Chem Phys 114:4171
90. Wetzig D, Rutkowski M, Ettrich W, David R, Zacharias H (1996) Rotational alignment in associative desorption of H_2 from Pd(100). Surf Sci 402:232